Vibrational energy redistribution in glyoxal following internal conversion

R. Naaman,[a] D. M. Lubman, and R. N. Zare

Department of Chemistry, Stanford University, Stanford, California 94305
(Received 4 June 1979; accepted 10 August 1979)

The vibrational redistribution of energy following internal conversion in glyoxal has been studied in a molecular beam using the "pump-and-probe" technique. A beam of glyoxal is initially pumped from S_o to a selected vibronic level of S_1. After internal conversion occurs, a tunable dye laser is used to probe the hot band absorption of the molecules by re-excitation into S_1. The total fluorescence as a function of probe laser wavelength is observed. The excitation spectrum is broad and featureless in the red but shows sharp structure in the vicinity of the pump laser wavelength. However, the sharp structure depends on the portion of the rotational contour excited. The experimental results show that the redistribution of energy is nonstatistical among the isoenergetic levels. This is explained by assuming that combination bands of low quanta of vibrations are the accepting levels in the internal conversion process and that these accepting levels undergo slow energy redistribution.

The current understanding of molecules having a high degree of vibrational excitation is incomplete. For energies near the ground state the molecular motions will be quasiperiodic; each trajectory is related to the next by using low-order perturbation theory to include effects of anharmonicity. The energy stays almost completely in the initial combination of excited normal modes. For energies far above the ground state, the molecular motion becomes quasiergodic; for sufficiently large time intervals the trajectories are uncorrelated and energy flows rapidly among the modes. The former regime is quantum mechanical (or classical); the latter regime is stochastic and a statistical description is the more appropriate.[1] The transition between the quasiperiodic and the quasiergodic regime is not sharp.[2,3] An outstanding question is to find the conditions, if any, for which the intramolecular exchange of energy is slow compared to other processes such as photon re-emission, isomerization, fragmentation, or subsequent chemical reaction. Based on the successes of RRKM theory[4] to account for the unimolecular decomposition rates of energized molecules, it is commonly held that vibrational energy is rapidly randomized relative to all other processes at total energies for which the vibrational level density is large.

In the present work we used the "pump-and-probe" technique[5] to study vibrational energy redistribution in the high vibrational levels of the electronic ground state (S_0), following internal conversion in glyoxal (CHOCHO). Glyoxal was chosen because its spectroscopy and radiative properties are well known.[6–16] Under collisionless conditions no intersystem crossing ($S_1 \sim T_1$) is detected,[8,9,11] and no photochemistry occurs.[9,13,14] The lifetimes of the vibrationless level and the 8^1 level are 2.4 and 0.87 μs, respectively,[11(a)] compared to the calculated radiative lifetime of 2.6 to 15 μs.[11(a),(b)] Therefore, more than 50% of the energy in S_1 is transferred to the ground state by internal conversion. In the case of glyoxal we find that although the molecule has about 22,000 cm^{-1} of energy in excess of the ground state, and a vibrational level density of about $10^8/cm^{-1}$ at this energy, the distribution of internal energy is distinctly nonstatistical among the isoenergetic vibrational levels.

EXPERIMENT

Figure 1 shows a schematic of the experimental setup. The molecular beam machine consists of a stainless steel cross to which a differentially pumped excitation/detection vacuum chamber is attached. Inside the cross is the beam source, which consists of a stainless steel tube terminating in a 25 μ glass capillary array. This array allows us to maintain a large flux of molecules ($\sim 1.5\times10^{15}$ molecules cm^{-2} sec^{-1}) while remaining within the effusive regime.

The glyoxal (Sigma Chem. Co.) was obtained in the form of a trimeric dihydrate. Before each experiment, glyoxal monomer was produced by heating the trimer in the presence of P_2O_5.[11] The product was distilled directly under vacuum into a large trap kept in dry ice–acetone. Then the trap is connected to the beam source tube (see Fig. 1). During the experiment the trap is immersed in ice water to prevent polymerization. The glyoxal pressure is controlled by a needle valve between the trap and the tube.

The effusive beam of glyoxal is defined by a collimating hole. A liquid-nitrogen-cooled trap is placed close to the collimation region to remove the scattered glyoxal molecules. In order to stay within the effusive limit the back pressure is maintained below 0.5 Torr, as measured by a Barocel capacitance manometer. The pressure in the chamber is measured by an ionization gauge. The density of molecules in the beam can be calculated from the flux. It is typically less than 7×10^{10} molecules cm^{-3}. This density divided by four gives the "effective density" which describes the collisional frequency. Under our conditions the average time between collisions in the beam is on the order of a second (effective pressure $\leq 8\times10^{-7}$ Torr). Therefore, we speak of the glyoxal molecules in the beam as isolated, i.e., in a collisionless environment.

Inside the excitation/detection chamber, the beam of

[a] Present address: Department of Chemistry, Harvard University, Cambridge, MA 02138.

 0021-9606/79/234192-09$01.00

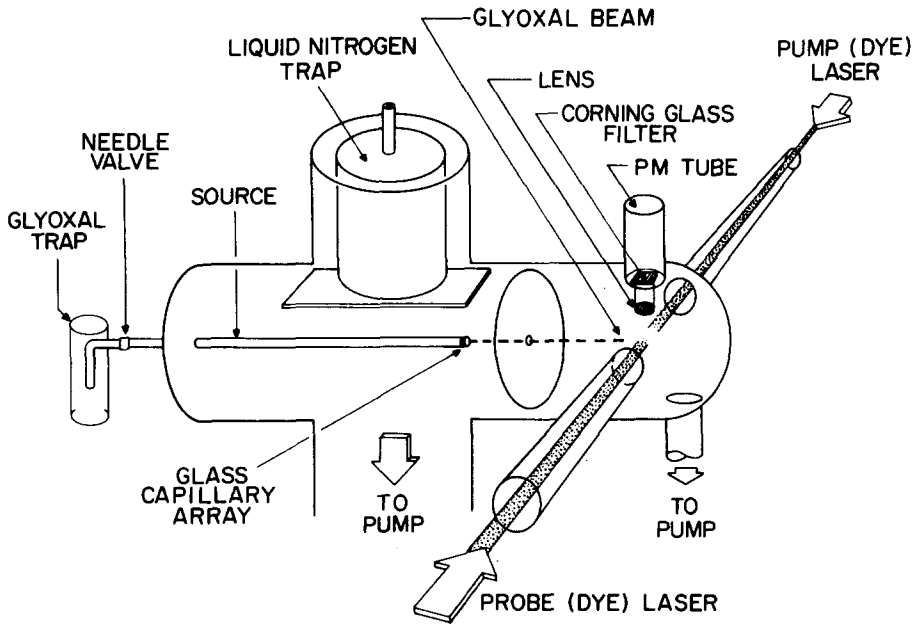

FIG. 1. Laser pump-and-probe setup for studying internal conversion in isolated glyoxal molecules.

glyoxal is pumped by a laser tuned to a vibronic transition ($S_0 \rightarrow S_1$). A second laser beam directed antiparallel to the first is tuned to a hot band of the glyoxal molecule. By observing the total undispersed fluorescence induced by the probe beam as a function of its wavelength, the energy redistribution is studied.

The excitation source used initially in this study was the 4545 Å line of a cw argon ion laser (CR2 Coherent Radiation, ~40 mW), which pumps the 0-0 band of the $S_0 \rightarrow S_1$ transition. The probe laser was a scannable nitrogen pumped dye laser (Avco N_2 laser, Molectron DL100 dye laser). The signal is very sensitive to the alignment. In order to observe a signal the two laser beams either are aligned collinearly in space or the probe beam is displaced along the direction of the molecular beam with respect to the pump beam. The latter arrangement maximizes the signal. Because of the use of long baffle arms to minimize the scattered light, the displacement was limited to only a few millimeters. The use of a cw laser in this experiment has the disadvantage that cw radiation produces a constant fluorescent background which decreases the S/N ratio. The use of a pulsed laser allows one to gate out the fluorescent background and the scattered light.

In our second series of experiments we initially used a home-built nitrogen pumped dye laser with a bandwidth of 0.5 Å. Later we used a commercial Nd:YAG pumped dye laser system (Quanta-Ray). This system can provide high power with a narrow bandwidth. At 440 nm (dye Coumarin 440) typically 2 mJ can be produced with a bandwidth of 0.2 cm^{-1}. The pump laser pulse starts a delay generator which triggers the probe laser (Fig. 2). The delay time between the two lasers is typically set between 0.7–1.2 μsec. In some experiments the delay was extended to 5 μsec.

We observe the fluorescence using an EMI 6256S photomultiplier located perpendicular to the laser beams and to the molecular beam. In order to increase the efficiency of the light collection a lens ($f/0.8$) images the interaction zone on the photomultiplier face. For broadband detection various glass cutoff filters are placed before the photomultiplier in order to reduce the scattered light.

The output of the photomultiplier feeds into a boxcar integrator (Princeton Applied Research Model 162 mainframe with a model 164 plug-in). The photomultiplier output can also be connected to the boxcar through a wide-band preamplifier (PAR model 115) when the signal level is low. The boxcar is triggered by the delay generator. The signal is maximized for very short lifetimes by triggering the gate simultaneously with the second laser. The gate width used was 5 nsec, since the

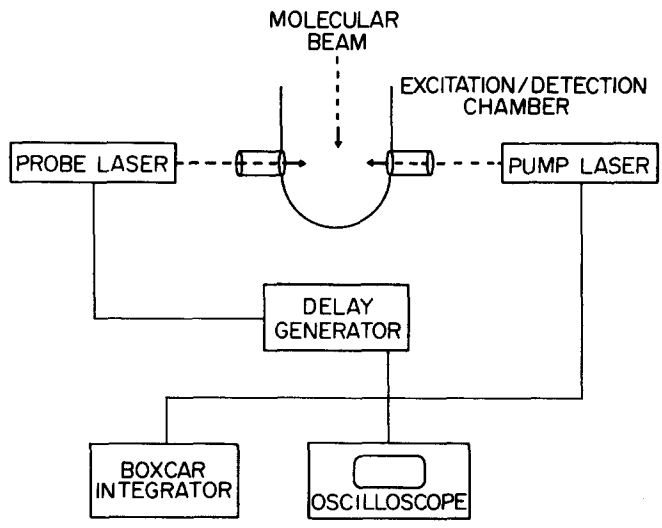

FIG. 2. Timing circuitry for controlling the delay between the pump and probe laser pulses. The pump laser triggers the delay generator and the gated detection electronics.

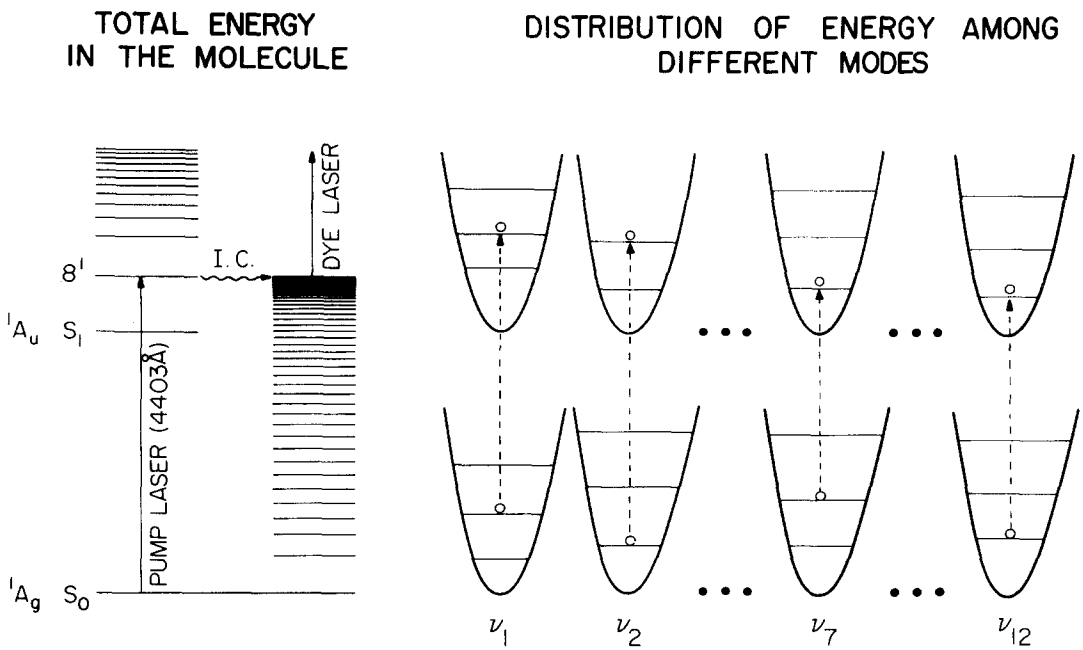

FIG. 3. The pump-and-probe scheme for determining the vibrational energy distribution in glyoxal following internal conversion. The total energy of the molecule is illustrated on the left, while one possible distribution of energy among the normal modes is shown on the right. In the latter the vertical arrows illustrate a transition induced by the probe laser.

induced fluorescence by the probe laser has a comparable lifetime.

RESULTS

Figure 3 illustrates the pump-and-probe technique for studying internal conversion in isolated glyoxal molecules. The pump laser prepares the molecule in a specific vibronic level of S_1. The present experiments select either the origin or the 8^1 level. The probe laser provides an additional energy of about 2 eV to the molecule. We observe the emission following the probe laser excitation. This emission has a significantly shorter lifetime (in the nanosecond regime) than the fluorescence from glyoxal induced by the pump laser. By using Corning filters we determined that the emission spectrum has crudely the same wavelength dependence as the fluorescence from S_1 excited by the pump laser. Signal-to-noise limitations prevented us from further dispersing the emission spectrum with the present setup. We conclude that the emission corresponds to transitions from high vibrational levels of S_1 to S_0. By high vibrational levels we mean those in which the molecule has high energy content. This can be achieved by deposition of the energy in high overtones or combination bands (see Fig. 3). At total energies in excess of 4 eV, the glyoxal molecule may isomerize or dissociate, but we rule out that an excited photofragment is responsible for the observed emission.

Figure 4 shows the excitation spectrum in the region of the origin obtained using the cw argon ion laser (4545 Å) as the pump laser. The same spectrum results using a pulsed dye laser tuned to the same wavelength as the pump source. The upper trace [Fig. 4(a)] shows the excitation spectrum when the pump laser is off. It has the same appearance as seen previously.[16] When the pump laser is turned on, the peak of the (0, 0) excitation spectrum falls and a new sharp feature rises near the pump laser wavelength [Fig. 4(b)]. As the background pressure in the excitation/detection chamber is increased [Figs. 4(c), (d)], the (0, 0) peak is restored and the new sharp feature decreases. To shorter wavelengths (Fig. 5) the excitation spectrum is highly structured, while at longer wavelengths (Fig. 6) a broad, weak featureless spectrum appears.

The signal to noise is significantly increased when a broad band (0.5 Å bandwidth) pulsed dye laser is used to pump the 8_0^1 transition[17] at 4403 Å. The improvement is caused by the efficiency of the internal conversion process from this level ($\tau_{f1} \sim 0.87$ μsec). In this case a sharp spectrum is observed also to the red of the pump frequency (Figs. 7 and 8). Further to the red, once again a broad and unresolved excitation spectrum appears (Fig. 9) whose shape changes with increasing background pressure.

Studies were also made using a narrow band (0.2 cm^{-1}) dye laser as the pump source. We found a strong dependence of the sharp features on the laser wavelength as it is tuned over the rotational contour of the 8_0^1 band (Fig. 10). The sharp structure can be made to disappear [Fig. 10(b)], although no significant effect was observed either in the red portion of the excitation spectrum or in the total fluorescence intensity induced by the pump laser.

Over the range that we are able to delay the probe laser (0.7 to 5 μsec) with respect to the pump laser, we observe no change in the form of the excitation spectrum within our signal to noise.

It might be thought that the repopulation of low vibrational levels of S_0 following fluorescence from the ini-

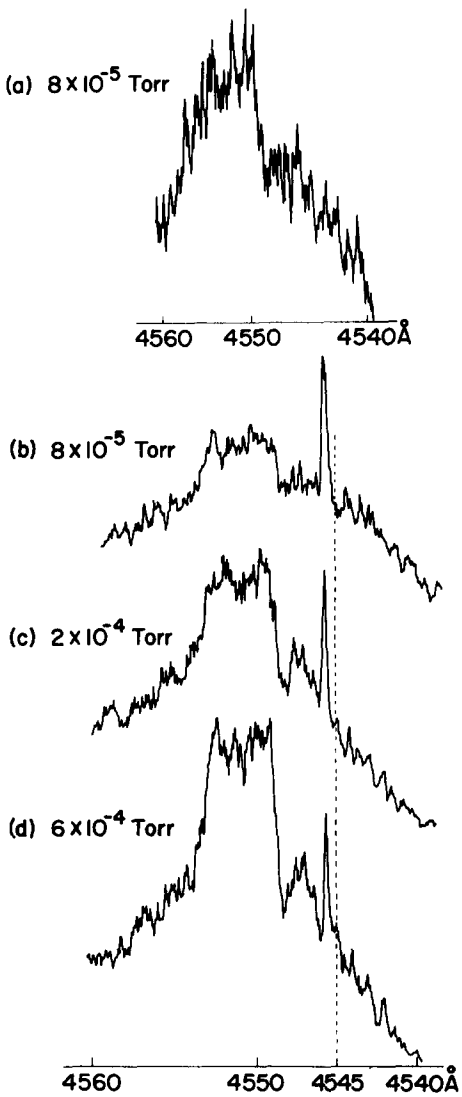

FIG. 4. Excitation spectra in the region of the origin obtained using a cw argon ion laser (4545 Å) when (a) the pump laser is off, (b)–(d) when the pump laser is on and when the excitation/detection chamber has different background pressures. In (b)–(d) the position of the pump laser wavelength is marked by a dashed line. The sharp feature to the red cannot be identified with certainty.

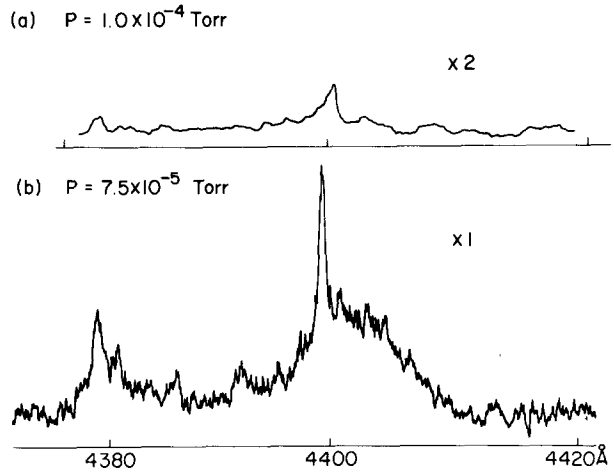

FIG. 5. Excitation spectra to the blue of the pump laser (4545 Å) when the pump laser is (a) off and (b) on.

tially prepared excited level of S_1 contributes in a major way to the observed excitation spectrum. By comparison with the known fluorescence spectrum[12] from 8^1, it was established that some contribution from this process may occur around 4617 and 4580 Å, but no contribution could be found to the red of these lines.

The present experimental configuration is not ideal for measuring pressure effects on the fluorescence emission. Nevertheless we observe significant variation in this signal by changing the background pressure in the excitation/detection chamber and the density of molecules in the effusive beam (Figs. 4 and 9). A quantitative determination cannot be made for the cross section for collision-induced energy redistribution. However we estimate that this cross section is quite large, on the order of 500 Å^2. Thus, this collision-induced process can be important even at pressures as low as 1 mTorr. At the lowest background pressures and beam fluxes we observe no collision-induced change in the excitation spectrum. Cross sections of similar size have been reported previously for other polyatomic molecules,[18,19] suggesting that this effect might be a common phenomenon. Not only must one take account of collision-induced energy redistribution in the intepretation of many studies of radiationless transitions but we suggest that it may also play a significant role in understanding many infrared multiphoton absorption processes.[20]

DISCUSSION

The laser pump-and-probe technique has been used to investigate the internal conversion of isolated glyoxal molecules in real time. This technique is quite general

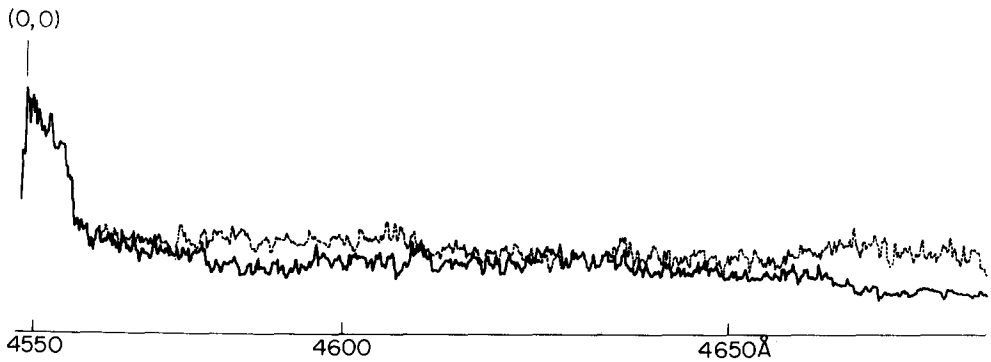

FIG. 6. Excitation spectra to the red of the pump laser (4545 Å) when the pump laser is off (lower trace) or on (upper trace). The difference between the two traces is small but reproducible.

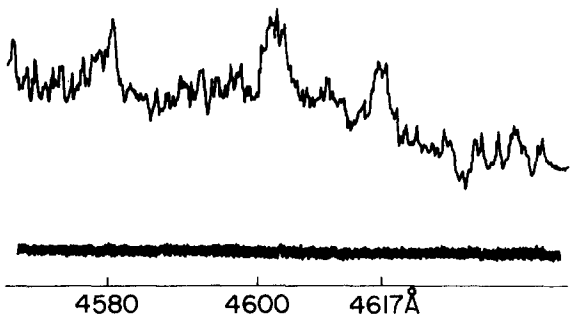

FIG. 7. Excitation spectrum in the region 4580–4617 Å is obtained using the 4403 Å pump laser. The lower trace is obtained when no pump laser is used.

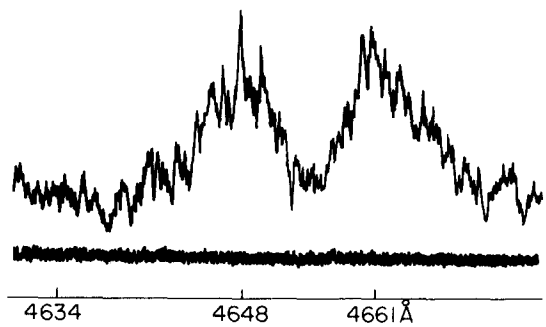

FIG. 8. Excitation spectrum in the region 4634–4661 Å is obtained using the 4403 Å pump laser. The lower trace is obtained when no pump laser is used.

and promises to open for more detailed study the photophysical behavior of molecules undergoing radiationless transitions. In particular, it can provide direct information on the nature of ground state molecules possessing high vibrational energy content.

The present study raises several questions concerning the nature of the internal conversion process and the subsequent fate of the internal energy:

(1) Why does the excitation spectrum show resolved features near the wavelength of the pump laser, although the density of vibrational levels is on the order of $10^8/\text{cm}^{-1}$?

(2) Why does the structured portion of the excitation spectrum change with pump laser wavelength?

(3) Why is the red shift of the excitation spectrum small relative to the absorption spectrum if the molecules are so "hot" (have such high internal energy content)?

(4) Why is the energy redistribution not equipartitioned among all isoenergetic levels, and why is it not completed on the time scale of our experiment (0.7–5 μsec)?

In the following discussion we attempt to answer these questions and present a model that provides a unified picture of the internal conversion and energy redistribution process. According to this model, energy flows from the initially selected vibronic level in S_1 to only a small subset of the manifold of isoenergetic vibrational levels in S_0 by internal conversion. Most of these energy levels are combination bands of low overtones. Each mode is populated to a small extent but the sum of the energies in each mode equals the energy initially deposited in the molecule. Because of the low quantum numbers for each vibration, the anharmonicity is not significant and energy does not transfer between modes during the time of observation.

The present understanding of internal conversion is still in flux and is a subject of much research activity.[21,22] However, a starting point for treating internal conversion in large molecules is provided by the Fermi golden rule expression for the rate[23]

$$k_{IC} = 2\pi/\hbar \left| V_{mv',nv''} \right|^2 \rho_n \,, \tag{1}$$

where ρ_n is the density of the vibrational levels in the ground state n and the matrix element, $V_{mv',nv''}$, connecting the excited state mv' to the ground state nv'' has the approximate form

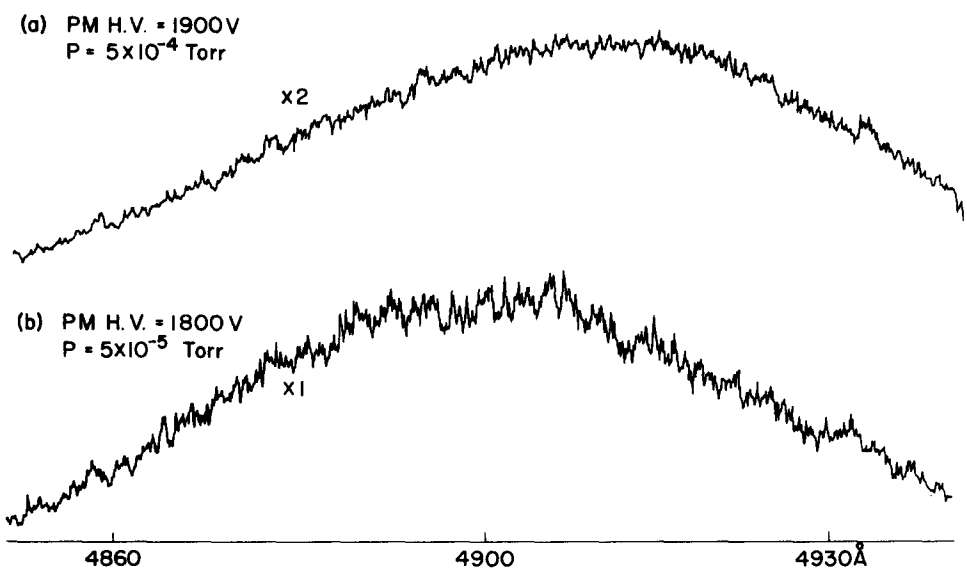

FIG. 9. Excitation spectra obtained in the red using the 4403 Å pump laser when the excitation/detection chamber is at different background pressures.

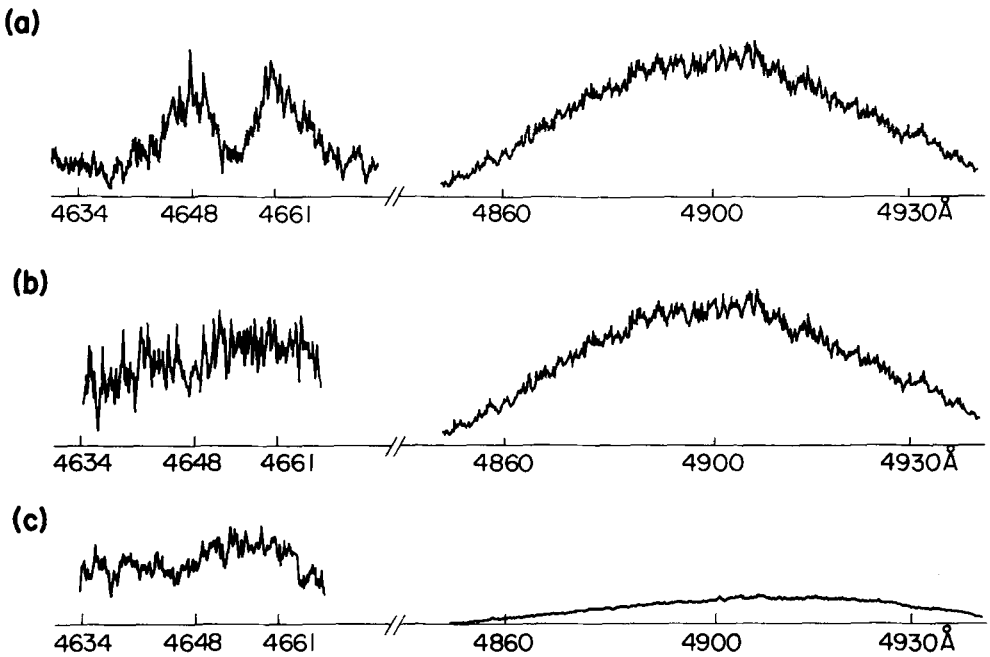

FIG. 10. Excitation spectra obtained using (a) broadband (1.5 cm^{-1}) pump laser at 4403 Å; (b) narrow band (0.2 cm^{-1}) pump laser tuned to one part of the rotational contour of the 8_0^1 transition (4403 Å); and (c) no pump laser.

$$V_{mv',nv''} \propto \sum_k \langle \Psi_m | \frac{\partial U(Q)}{\partial Q_k} | \Psi_n \rangle \times \langle \chi_{mv_k'} | \frac{\partial}{\partial Q_k} | \chi_{nv_k''} \rangle \prod_{i \neq k} \langle \chi_{mv_i'} | \chi_{nv_i''} \rangle \quad (2)$$

where the total wave function is written as the product of an electronic wave function $\Psi(q, Q)$ and a vibrational wavefunction $\chi(Q)$, and the summation is over all normal modes. As can be seen from Eq. (2), the vibronic energy in S_1 is not partitioned equiprobably among all isoenergetic levels in the ground state. Since the symmetry of S_1 is A_u and that of S_0 is A_g, only normal modes of a_u symmetry (called the promoting modes) contribute to the summation in Eq. (2). As Table I shows, there are two such modes, ν_6 and ν_7, of which the latter is believed to contribute more strongly. This is caused by the large change in frequency between S_1 and S_0 for ν_7 compared to ν_6.[11] Finally, the Franck–Condon principle [see the last term in Eq. (2)] favors the energy being deposited in ground state levels having a large vibrational overlap with the excited level. Thus the internal conversion process initially selects only a small subset of the manifold of isoenergetic ground state levels.

After a time on the order of a microsecond, a probe laser interrogates the molecule. If the initial distribution of vibrational energy levels in S_0 does not undergo extensive energy redistribution, then structured features will appear in the excitation spectrum in the vicinity of the pump laser wavelength. Most of the modes have a lower vibrational frequency in S_1 than in S_0 (see Table I). Therefore many of the combination bands will absorb energy which is red shifted relative to the pump laser wavelength. Indeed, only a limited number of combination bands can absorb energy in the wavelength region near the pump laser and these combination bands must contain overtones of ν_7 and/or ν_{12} to offset the red shift of the other modes. Consequently, one expects to observe sharper structure in the blue than the red.

Let us consider in more detail the red shift in the excitation spectrum. In addition to the fact that the vibrational frequencies are lower on the average in S_1 than in S_0, there is another contribution to the red shift. As the vibrational quantum number v_k'' of mode k increases, transitions to $v_k' \neq v_k''$ become stronger. Thus the population of high overtones of a mode will cause more extensive red shifting than the population of combination bands having the same energy. In this experiment no strong signal could be observed when the probe laser is scanned over the wavelength region 5000–7000 Å. Because the excitation spectrum shows relatively small red shifting, we conclude that combination bands of low overtones are primarily responsible for accepting the energy, i.e., are the accepting levels.

In many theoretical treatments of radiationless processes, high overtones are assumed to accept the energy.[24,25] This study on glyoxal suggests a counterex-

TABLE I. Vibrational frequencies in glyoxal.[12]

Symmetry	Vibration	^1A_g	^1A_u
a_g	ν_1 C–H stretching	2 844	2 809
	ν_2 C=O stretching	1 745	1 391
	ν_3 C–H rocking	1 338	
	ν_4 C–C stretching	1 065	955
	ν_5 C–C=O bending	550	509
a_u	ν_6 C–H wagging	801	719
	ν_7 torsional	127	233
b_g	ν_8 C–H wagging	1 048	735
b_u	ν_9 C–H stretching	2 835	
	ν_{10} C=O stretching	1 732	
	ν_{11} C–H rocking	1 312	
	ν_{12} C–C–O bending	338	380

ample. Indeed, combination bands of low overtones may explain several outstanding puzzles. For example, in benzene it has not been possible to obtain a reasonable rate constant for intersystem crossing calculated by assuming a Lorentzian line shape of the overtone (accepting mode).[26] This is contrary to experimental results that show that the overtones have Lorentzian line shapes.[27] The contribution from combination bands as accepting levels may reconcile this discrepancy. This may also explain the small deuteration effect observed in the radiationless processes of some polyatomic molecules, whereas calculations in which overtones are primarily the accepting modes predict isotope effects that are too large.[28]

The change of the structured portion of the excitation spectrum with pump laser bandwidth points to a rotational dependence of the radiationless process. This may be caused by (a) different vibrational levels of S_0 coming into resonance with the rovibronic level of S_1 at different excitation energies and (b) a rotational dependence of the internal conversion rate. The latter cannot be seen in Eq. (2) which was derived by assuming that the projection of the rotational angular momentum on the molecular top axis is constant. Rotational dependence of radiationless transitions has been observed previously in several other molecules.[19,29,30]

Based on the RRKM theory the vibrational energy redistribution rate is expected to be proportional to the density of vibrational levels. At the pump energy in this experiment (~22 000 cm^{-1}), the vibrational level density is so high (about $10^8/cm^{-1}$) that it might be supposed that the internal energy is statistically distributed among all isoenergetic levels even though the internal conversion process selectively deposits energy in a few levels. Moreover, the energy redistribution should occur rapidly, i.e., on the order of picoseconds, giving a width to each accepting level.

To test this picture a computer program was written that determined the spectral transition for each isoenergetic level in the range of the excitation spectrum where signal was observed (see Appendix). Some simple approximations were made. Each level was assumed to have a width of 1 cm^{-1}. Only $\Delta v = 0$ transitions were allowed. Possible contributions from *cis*-glyoxal to the excitation spectrum in this region were neglected since the region[31] is shifted to the red (4875 Å). Figure 11 presents the computer simulated excitation spectrum.

A comparison of Fig. 11 with Figs. 7 and 8 shows that this model is unable to reproduce our observations. This conclusion still holds if $\Delta v = \pm 1$ transitions are also included. We take this as a demonstration that part of the energy following internal conversion is *not* statistically distributed among all isoenergetic levels, even after several microseconds have elapsed. Not only is the presence of sharply structured features evidence for nonstatistical energy redistribution but the fact that these features depend sensitively on the pump wavelength also supports this conclusion. In diatomic molecules the total energy can be uniquely associated with the extent of vibrational excitation. However, in polyatomic molecules there are a large number of combinations of vibrations with the same total energy. Therefore, if the pump-and-probe experiment is viewed only in terms of the total energy (left side of Fig. 3), this might cause confusion. In this study of internal conversion in glyoxal we believe that the total energy deposited in the molecule is distributed mainly among combination bands of low overtones (right side of Fig. 3). Moreover, it is these combination bands that are responsible for the structured features in the excitation spectrum and it is their low anharmonicity that explains the incomplete energy redistribution that is observed. This study may be the first instance where quasiperiodic levels at high vibrational energies have been experimentally detected. It may be possible in the future to assign these structured features. The computer program we have written already is able to predict the location of such features within a few reciprocal centimeters of where they are found. If this possibility is realized, then the high vibrational levels of ground state molecules are opened for spectroscopic study.

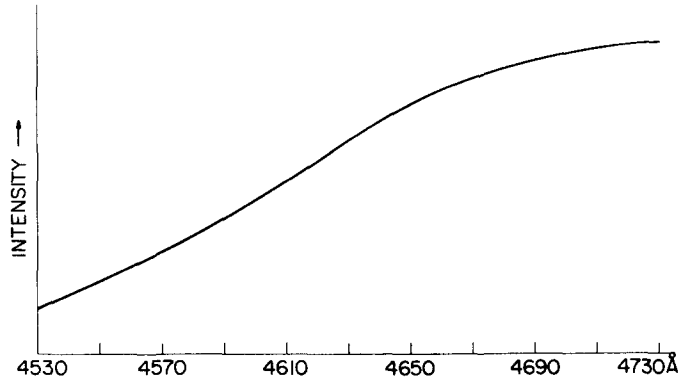

FIG. 11. Simulated excitation spectrum for glyoxal assuming the energy of internal conversion is partitioned statistically among the isoenergetic levels (see Appendix). When the density of transitions exceeded 15 per reciprocal centimeter, the spectrum was taken as structureless within this region.

ACKNOWLEDGMENTS

We are grateful to J. McGrath who wrote and executed the computer program. The assistance of I. Shiluach in developing the counting algorithm is much appreciated. We also thank G. H. Atkinson for making available to us unpublished data on glyoxal fluorescence and the Stanford Center for Materials Research for loan of a Nd : YAG laser. This work was supported by the National Science Foundation.

APPENDIX: COMPUTER SIMULATED EXCITATION SPECTRA OF VIBRATIONALLY EXCITED POLYATOMIC MOLECULES

This appendix describes a computer program used to generate an excitation spectrum for a polyatomic molecule having a vibrational energy E_V. The program counts and identifies all levels having the energy E_V. Then the absorption spectrum is calculated based on a knowledge of the upper and lower state vibrational frequencies. This program is general. However, in what follows we restrict the discussion to internal conversion

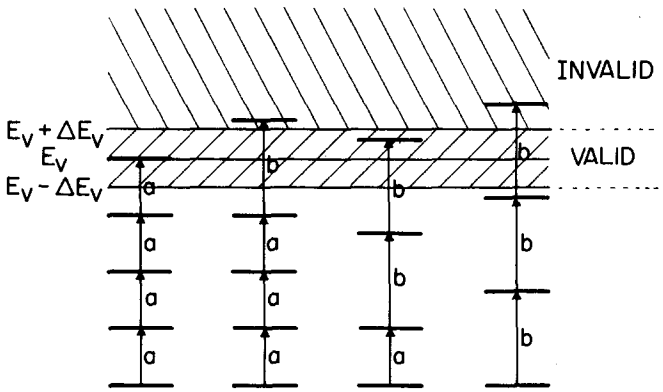

FIG. 12. Counting algorithm for determining the combination of overtones falling within $E_V \pm \Delta E_V$. Two fundamentals, a and b, are illustrated (see text).

in the glyoxal molecule. The excitation spectrum is calculated for two limiting cases: (a) complete energy redistribution among all isoenergetic levels; and (b) no energy redistribution.

A search is made for combinations of vibrational modes $\nu_1, \nu_2, \ldots, \nu_{12}$ having the energy E_V. The frequencies are ranked in ascending order. The program adds the lowest frequency to itself until the sum, E_T, equals or exceeds E_V within the range ΔE_V. Those combinations with

$$E_V - \Delta E \leq E_T \leq E_V + \Delta E \qquad \text{(A1)}$$

are judged as valid. Then the program subtracts the two quanta of the lowest frequency and adds the next lowest frequency. The program continues to subtract quanta of the lowest frequency and add quanta of higher frequencies until all possible combinations satisfying (A1) are found. Figure 12 illustrates this search procedure for the simple case of two unequal frequencies.

The above search procedure becomes quite time consuming as E_V increases in size. We limited the search to those combinations whose overtones of modes does not exceed some set number. This restriction corresponds to rejecting combinations that have highly unfavorable vibrational overlap with the initially excited level in S_1 [see Eq. (2)].

In the case of glyoxal, some of the frequencies are unknown in S_1 (see Table I). For these modes we assumed no frequency change. The program assumes harmonic behavior; anharmonic corrections can easily be added, if known. In simulating the excitation spectrum shown in Fig. 11, the pump laser was assumed to have a bandwidth of 3 cm^{-1} and the excitation spectrum a resolution of 1 cm^{-1}.

The program also lists the transitions that occur in some chosen energy range of the spectrum. This permits tentative assignments to be made. For example, consider the structured feature at 4580 Å in Fig. 7, which lies 150 cm^{-1} to the red of the origin. As stated before, only combinations with odd quanta (overtones) of ν_7 and/or ν_6 can be accepting levels according to symmetry. With the assumptions that ν_7 is the promoting mode, only one quanta of ν_7 is populated, and $\Delta v = 0$ transitions dominate the excitation spectrum, the program finds the following possible transitions between 144–150 cm^{-1} from the origin:

1_5^5	3_1^1	7_1^1	10_1^1	11_3^3	12_4^4	
1_1^1	2_1^1	3_2^2	7_1^1	9_4^4	11_2^2	12_4^4
3_4^4	4_2^2	5_3^3	6_2^2	7_1^1	9_3^3	11_1^1 12_6^6
1_1^1	3_4^4	4_1^1	7_1^1	8_1^1	9_2^2	11_4^4 12_4^4
1_4^4	2_1^1	3_1^1	7_1^1	9_1^1	11_3^3	12_4^4
1_2^2	4_1^1	5_1^1	7_1^1	9_4^4	11_3^3	

of these, the last one may have the largest vibrational overlap for internal conversion. If no symmetry restrictions had been placed, one obtains about 30 transitions per cm^{-1} in the excitation spectrum at 4580 Å and no sharp features result.

[1] K. S. J. Nordholm and S. A. Rice, J. Chem. Phys. 61, 203, 768 (1974); 62, 157 (1975).
[2] D. W. Noid and R. A. Marcus, J. Chem. Phys. 67, 559 (1977).
[3] E. J. Heller, Chem. Phys. Lett. 60, 338 (1979).
[4] See P. J. Robinson and K. A. Holbrook, *Unimolecular Reactions* (Wiley, New York, 1972); W. Forst, *Theory of Unimolecular Reactions* (Academic, New York, 1973).
[5] R. K. Sander, B. Soep, and R. N. Zare, J. Chem. Phys. 64, 1242 (1976).
[6] C. S. Parmenter, J. Chem. Phys. 41, 658 (1964).
[7] J. T. Yardley, G. W. Hollman, and J. I. Steinfeld, Chem. Phys. Lett. 10, 266 (1971).
[8] L. G. Anderson, C. S. Parmenter, H. M. Polland, and J. D. Rau, Chem. Phys. Lett. 8, 232 (1971).
[9] L. G. Anderson, C. S. Parmenter, and H. M. Polland, Chem. Phys. 1, 401 (1973).
[10] R. van der Werf, E. Schutten, and J. Kommandeur, Chem. Phys. 11, 281 (1975).
[11] (a) R. A. Beyer, P. F. Zittel, and W. C. Lineberger, J. Chem. Phys. 62, 4016 (1975); (b) B. G. MacDonald and E. K. C. Lee, J. Chem. Phys. (to be published).
[12] G. H. Atkinson, R. A. Malstrom, and M. E. McIlwain, J. Mol. Spectrosc. 76, 164 (1979).
[13] E. Drent, R. P. van der Werf, and J. Kommandeur, J. Chem. Phys. 59, 2061 (1973).
[14] G. H. Atkinson, M. E. McIlwain, and C. G. Venkatesh, J. Chem. Phys. 68, 726 (1978). They report the formation of CO under collisional conditions (1 Torr or higher pressures) and suggest that collision-induced intersystem crossing precedes dissociation. Note that the possible photochemical products cannot absorb the probe laser wavelength.
[15] C. Michel and A. Tramer, Chem. Phys. 42, 315 (1979).
[16] W. Holzer and D. A. Ramsay, Can. J. Phys. 48, 1759 (1970).
[17] X_i^j denotes a vibronic transition from i quanta of vibrational mode X in the ground state to j quanta of the same mode in the excited state, where the normal mode X is defined in Table I.
[18] R. Naaman, D. M. Lubman, and R. N. Zare, Chem. Phys. 32, 17 (1978).
[19] J. C. Weisshaar, A. P. Baronavski, A. Cabello, and C. B. Moore, J. Chem. Phys. 69, 4720 (1978).
[20] See for example (a) F. M. Lussier, J. I. Steinfeld, and F. Deutsch, Chem. Phys. Lett. 58, 277 (1978); (b) I. P. Herman and J. B. Marling, Chem. Phys. Lett. (in press).
[21] W. Siebrand and M. Z. Zgierski, Chem. Phys. Lett. 58, 8 (1978).

[22](a) B. Scharf, Chem. Phys. 7, 478 (1975); (b) B. Scharf and R. Naaman, Chem. Phys. Lett. 59, 151 (1978).
[23]J. Jortner, S. A. Rice, and R. W. Hochstrasser, Adv. Photochem. 7, 149 (1969).
[24]R. Englman and J. Jortner, Mol. Phys. 18, 145 (1970).
[25]D. F. Heller, K. F. Freed, and W. M. Gelbart, J. Chem. Phys. 56, 2309 (1972).
[26]I. H. Kühn and F. Metz, Chem. Phys. 33, 137 (1978).
[27]K. V. Reddy, R. G. Bray, and M. J. Berry, General Discussion Meeting on Radiationless Processes, Breukelen, The Netherlands (1977), p. 146.
[28]C. V. Shank, E. P. Ippen, O. Teschke, and R. L. Fork, Chem. Phys. Lett. 57, 433 (1978).
[29]V. Boesl, H. J. Neusser, and E. W. Schlag, Chem. Phys. Lett. 31, 11 (1975).
[30]K. Shibuya and E. K. C. Lee, J. Chem. Phys. 69, 5558 (1978).
[31]G. N. Currie and D. A. Ramsay, Can. J. Phys. 49, 317 (1971); R. A. Beyer and W. C. Lineberger, Chem. Phys. Lett. 20, 600 (1973). *Cis*-glyoxal may contribute to the excitation spectrum at wavelengths longer than 4875 Å. The *cis*-glyoxal may be formed by isomerization in S_0 following internal conversion.